



The Thermoelectric Transport Properties of Tin Selenide From First-Principles Calculations

B C. Oyomo* P W Muchiri # and G O. Amolo

*billclintone44@gmail.com

#pshiroh2015@gmail.com

Materials Modeling Group, School of Physics and Earth Science,
The Technical University of Kenya.

Introduction

- Thermoelectricity is the direct conversion of heat into electricity and vice versa, i.e. Seebeck and Peltier effect.
- Seebeck effect – phenomenon in which temperature difference creates an electric potential: used in thermoelectric generators (TEGs).
- Peltier effect – is the evolution or absorption of heat at the junctions of two dissimilar materials due to a potential difference.
- The efficiency of the thermoelectric materials is determined by dimensionless figure of merit given by
$$ZT = \frac{S^2 \sigma T}{K_e + K_l}$$
- S is the Seebeck coefficient, σ is the electrical conductivity, T is the operating temperature, K_e and K_l are the electron and lattice thermal conductivities, respectively.
- For high ZT a thermoelectric material should have:
 - high Seebeck coefficient (S)
 - high electrical conductivity (σ)
 - low thermal conductivity ($K_e + K_l$)

Thermoelectric devices and Applications

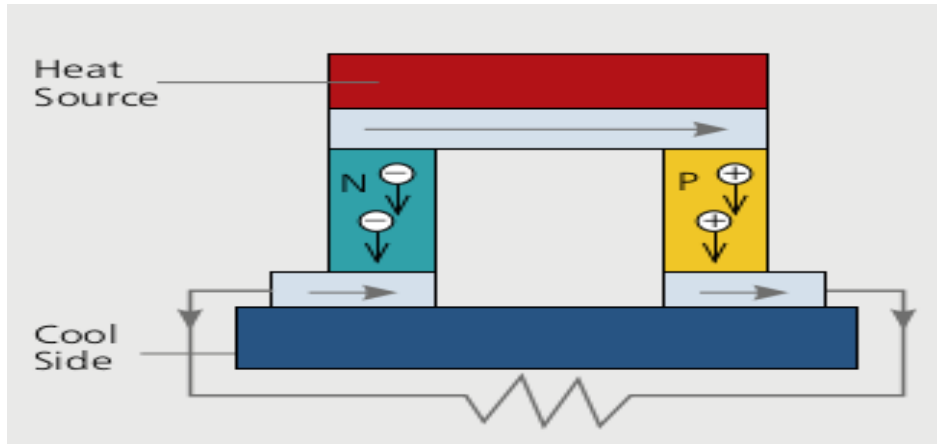


Fig.1 TEG setup

Thermoelectric Generator (TEG) working principle

- Temperature gradient causes charge diffusion from the hot to cold side.
- A potential difference is created and consequently current flows.
- Applications: Radioisotope TEG in deep space probes

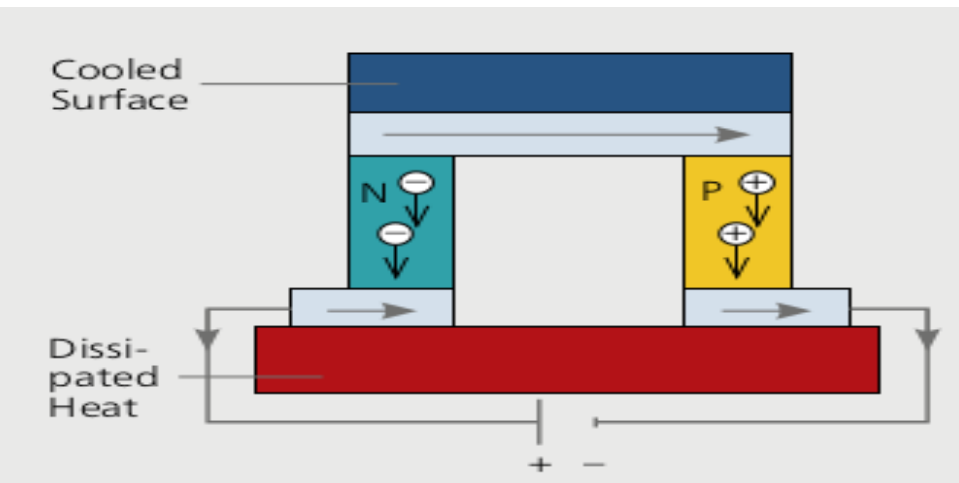


Fig.2 TEC

Thermoelectric Cooler (TEC)

- Current is applied in the setup, heat is absorbed at one end and evolved at the other end creating a temperature gradient
- Applications: IR detector cooling, laser frequency stabilization, automotive seat temperature control, etc.

Why Tin Selenide (SnSe)?

- Lead chalcogenides are the best TE materials at mid-high temperatures while Bismuth chalcogenides perform best at room temperature (Kumar et al., 2016). However, lead is toxic limiting large scale application while Bismuth and Tellurium are expensive.
- Tin Selenide (SnSe) which is lead free hence non-toxic and composed of relatively abundant elements could be an ideal alternative for thermoelectric applications.

Objectives

- i. To calculate the band structure and Projected density of states (pdos) of SnSe.
- ii. To determine the electrical conductivity of SnSe.
- iii. To calculate the electron thermal conductivity of SnSe.
- iv. To determine the Seebeck coefficient of bulk SnSe.

Methodology

- Package: Quantum Espresso code for electron structure calculations to implement Density Functional Theory (DFT) (Giannozzi et al., 2009).
- Functional: Generalized Gradient Approximation (GGA) in the form of Perdew-Burke-Enzerhof (PBE) exchange correlation functional was used.
- Ultrasoft Pseudopotentials for treating the Sn & Se valence electrons (Kresse & Joubert, 1999).
- Kinetic energy cut off was set to 80 Ry. The Brillouin zones were integrated by $2 \times 10 \times 10$.
- The thermoelectric properties were then calculated using BoltzTraP code that solved Boltzmann transport equation under constant relaxation time (Madsen & Singh, 2006).

Density Functional Theory

- Density functional theory (DFT) is a successful and widely used approach to determine the ground state properties of materials
- It is applied in atoms, molecules, solids etc
- DFT converts the many-body Schrodinger equation to non-interacting single particle equations.
- The resulting equations are called Kohn-Sham equations;

$$\left[\frac{-\hbar^2}{2m} \nabla^2 + V_{eff} \right] \psi_i(\vec{r}) = \epsilon_i \psi_i(\vec{r})$$

where V_{eff} is the effective potential given by; $V_{eff} = [V_{ext}(\vec{r}) + V_H(\vec{r}) + V_{XC}(\vec{r})]$

- Ψ_i and ϵ_i are the wave functions and energy of the non- interacting particles, respectively.
- V_{ext} , V_H and V_{XC} are the external, Hartree and exchange correlation potentials, respectively.
- These equations are solved and then the ground state properties computed.

Boltzmann Transport Equation

➤ Boltzmann Transport Equation (BTE) is given as ;

$$\frac{\partial f}{\partial t} + \vec{V} \cdot \nabla_r f + \vec{F}_e \cdot \nabla_p f = \frac{\delta f}{\tau} \quad \text{Where; } \tau \text{ is the relaxation time}$$

\vec{V} is velocity, \vec{F}_e is the Force, $\frac{\delta f}{\tau}$ is the scattering term (change in f due to scattering), $\nabla_r f$ and $\nabla_p f$ are gradient of f in space and gradient of f in momentum space, respectively.

➤ Generalized solution is given by ;

$$\delta f = \tau_m \left(\frac{-\delta f_0}{\delta E} \right) \vec{V} \cdot \vec{F}$$

➤ f is the distribution function out of equilibrium.

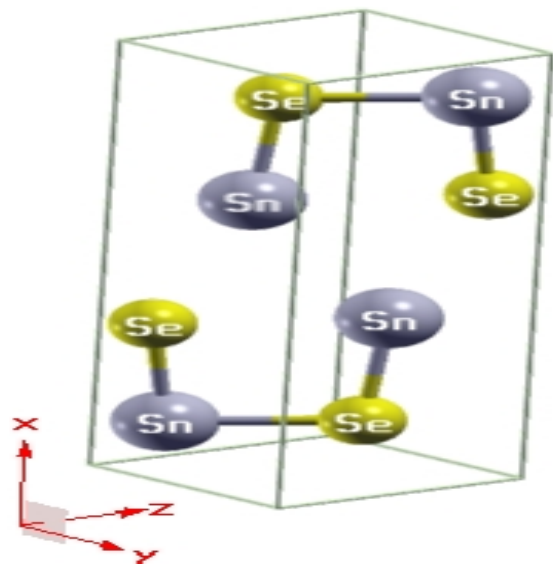
➤ f_0 is distribution function in equilibrium given by ;

$$f_0 = \frac{1}{1 + e^{(E - E_F)/K_B T}} \quad \text{where; } E \text{ is the total energy and } E_F \text{ is the Fermi energy}$$

➤ Solving the BTE gives f from which various transport quantities can be obtained.

Geometrical Structure of Tin Selenide

- Tin Selenide adopts an orthorhombic crystal structure at room temperature with 8 atoms per unit cell.
- The lattice parameters, bond angles and bond lengths obtained from this work are shown in the table below



	<i>Experimental</i>	<i>Theoretical</i>	<i>Deviation</i>
Lattice Parameters	A= 11.55 Å (2)	A= 11.80 Å	+0.25
	B= 4.16 Å (2)	B= 4.25 Å	+0.09
	C= 4.45 Å (2)	C = 4.50 Å	+0.05
Bond Lengths (Angstrom)	Sn-Se=2.833 Å (2)	Sn-Se= 2.8375 Å	+0.0045
	Se-Sn=2.774 Å (2)	Se-Sn= 2.7758 Å	+0.0018
Bond Angles (°)	-	Se-Sn-Se = 89.44°	-
	-	Sn-Se-Sn = 100.42°	-

Fig 3. optimised structure of SnSe

parameters, bond angles & bond lengths for SnSe

- The lattice constants are slightly overestimated compared to the experimental results. This is because the GGA tends to overestimate the lattice constants.

yx, xz and yz views of the structure of SnSe

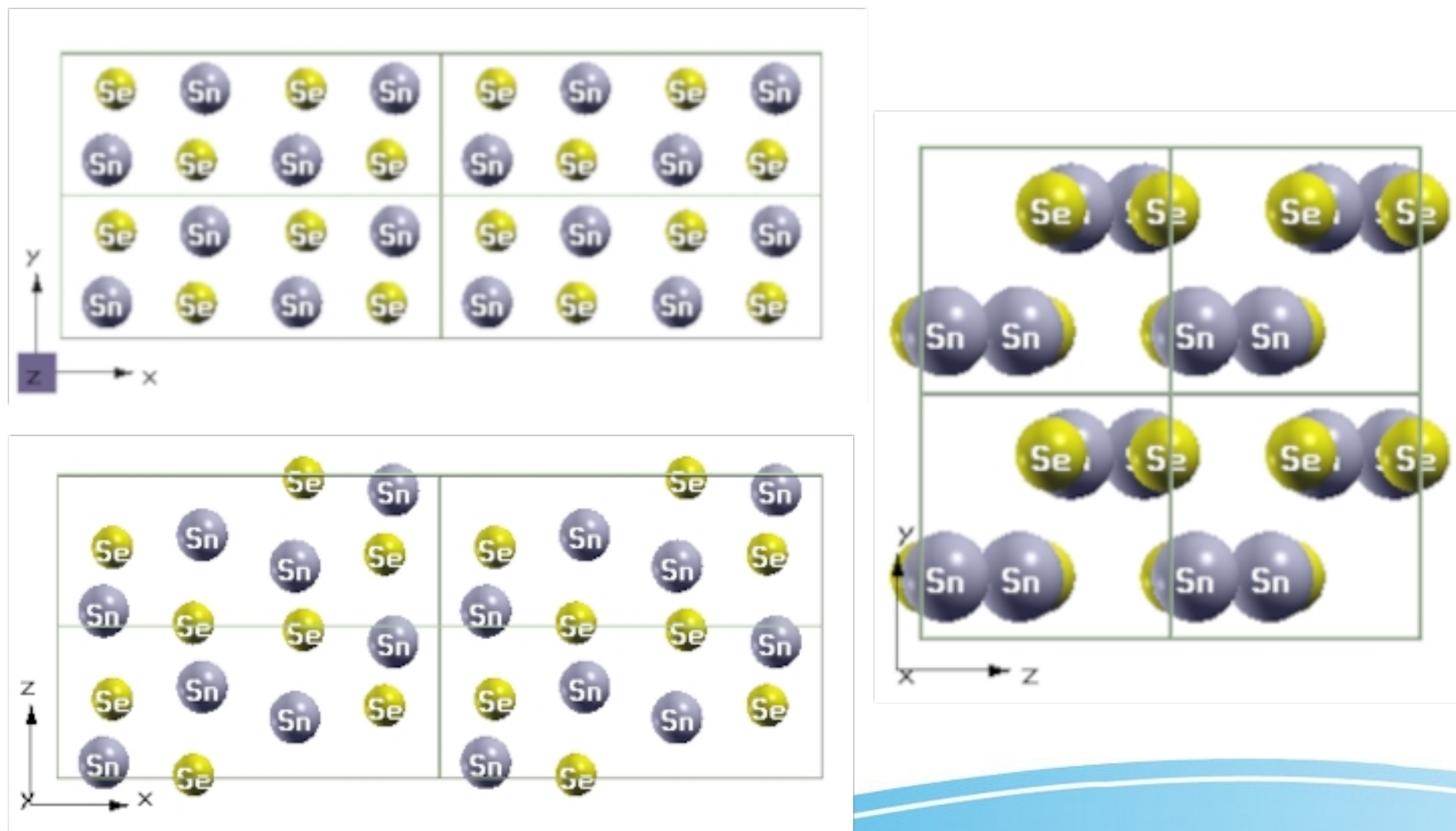


Figure 4. Structure of SnSe viewed from the 3 different planes

Band structure and Pdos

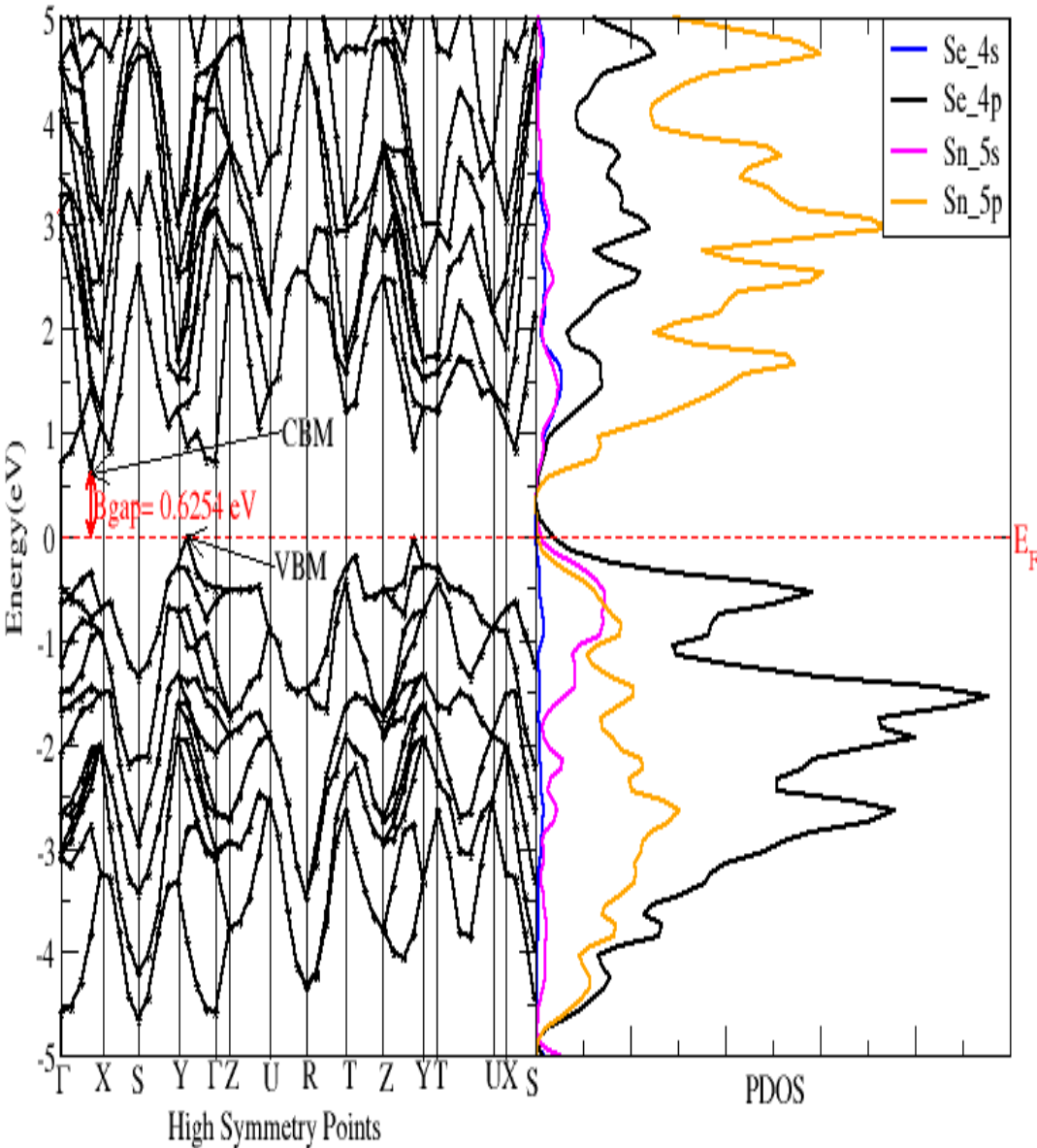


Figure 5. Band Structure and Pdos of SnSe

- An indirect band gap of 0.625 eV between Γ -X and Y- Γ high symmetry points. This suggests semiconducting properties.
- Se-4p orbital and the Sn-5p make up the valence band maximum and conduction band minimum, respectively.
- Experimental band gap value is 0.9 eV (Huang et al., 2017)
- The conduction band is mainly contributed by the Sn-5p and Se-4p states while the Sn-5s states have almost no contribution to the conduction band.
- Se-4p states are more dominant the valence band than the Sn-5p while the Sn-5s and Se-4s states offer very little contribution to the valence band

Electrical conductivity vs temperature

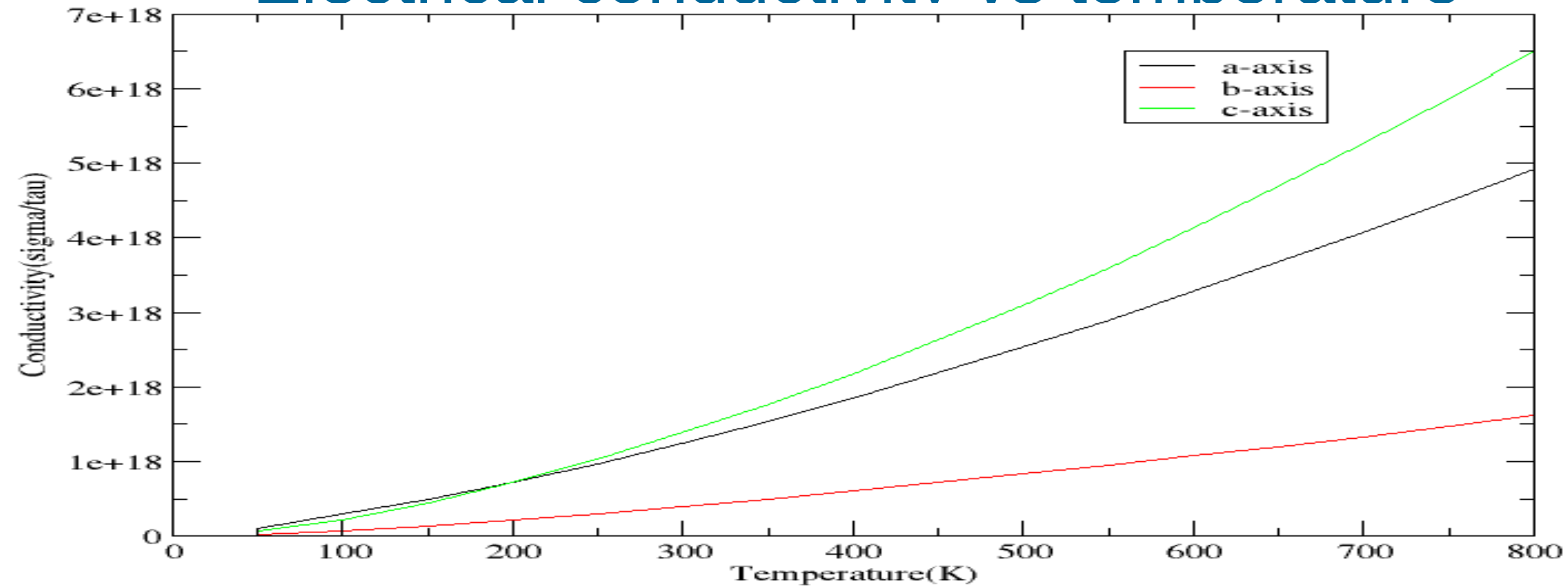


Figure 6. Graph of electrical conductivity Vs Temperature

- Electrical conductivity (σ) is high and increases significantly with rise in temperature on the a and c axes while the b-axis exhibits lower electrical conductivity that increases slightly with temperature increase.
- This anisotropy can be attributed to the high electron density along the a & c axes than the b axis hence a higher electron mobility on the ac-plane of SnSe compared to the bc-plane.
- These calculations were performed at temperatures between 50 K to 800 K, below the melting point of SnSe that is 1134 K.

Electron thermal conductivity vs temperature

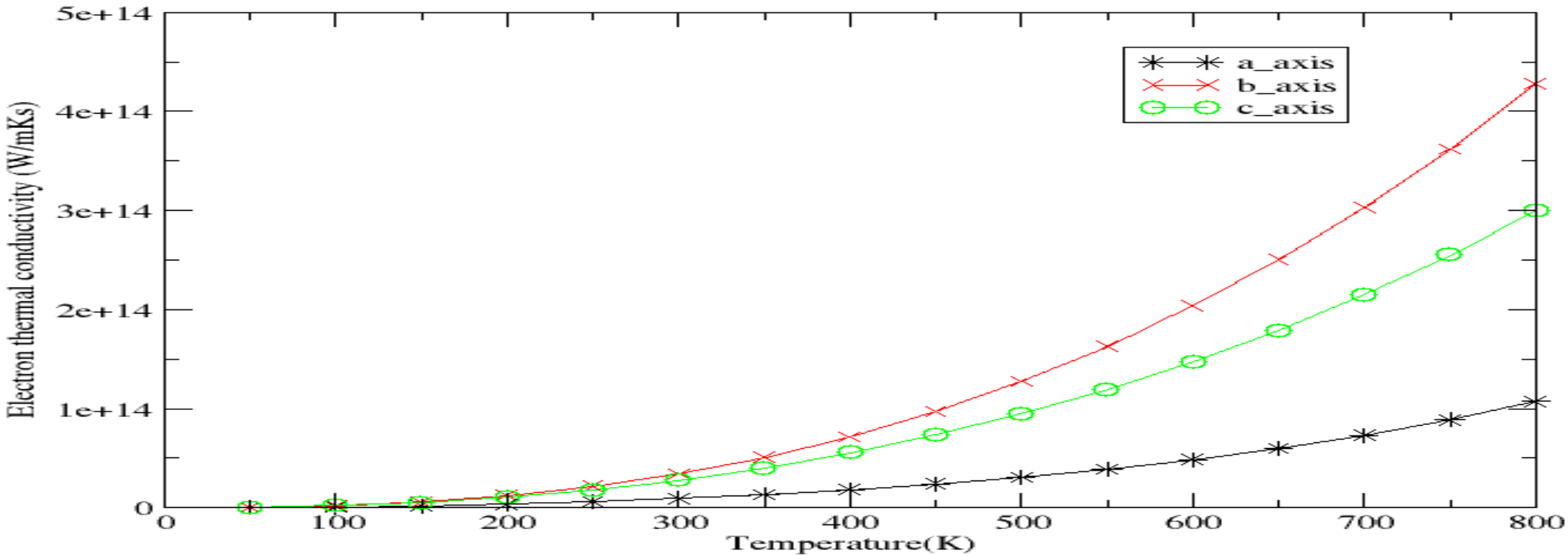


Fig 7. Graph of electron thermal conductivity vs Temperature

- Anisotropic electron thermal conductivity (K_e) is exhibited with b and c axes having higher electron thermal conductivity than the a axis. This may be due to the Higher electron density on the bc plane compared to the ac plane. Distribution of atoms on the planes shown in figure 4.
- The electron thermal conductivity increases with temperature on all crystal axes and is quite low compared to the electrical conductivity.

Seebeck Coefficient

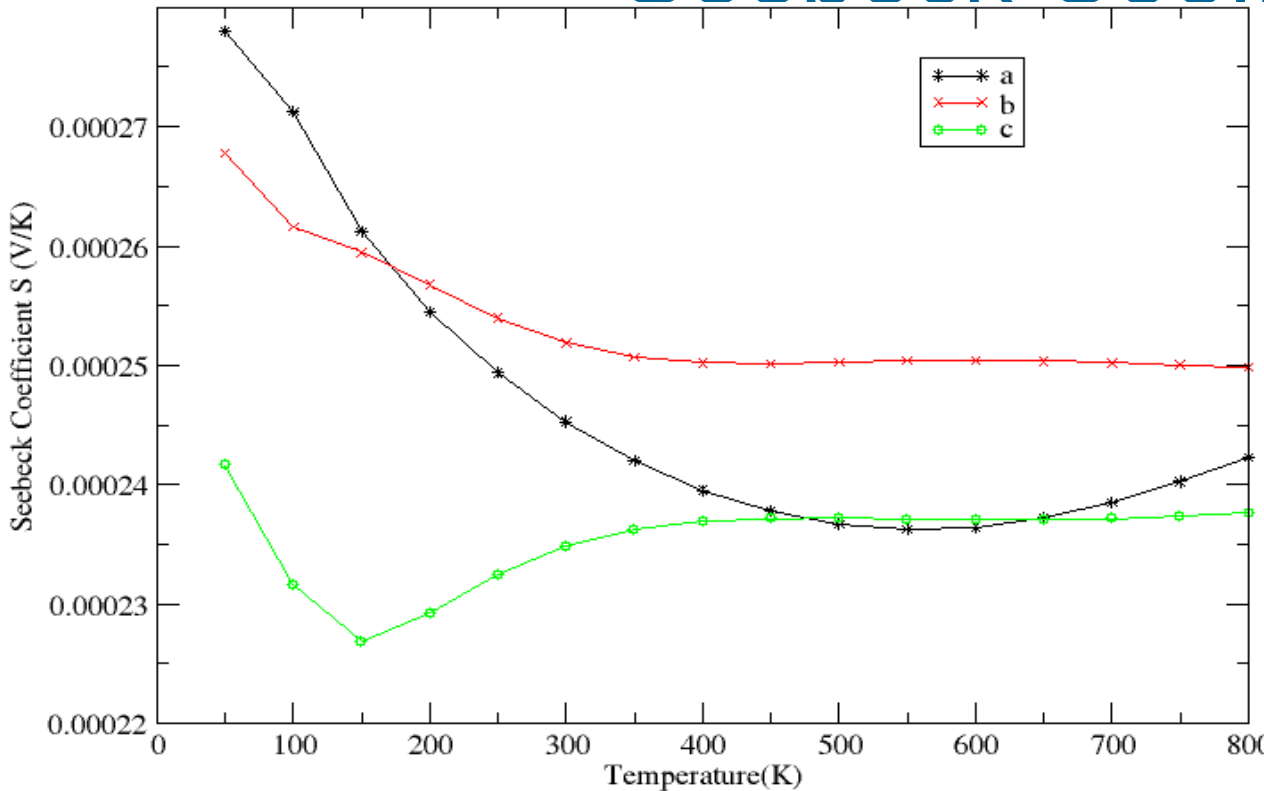


Fig 8. Seebeck coefficient Vs Temperature

Temperature (K)	300	600	800
Seebeck coefficient ($\mu\text{V/K}$)			
a	245.12	236.39	242.125
b	251.66	250.37	249.845
c	234.67	237.02	237.564

Table 2. Seebeck coefficient across a, b and c axes at different temperatures

- Seebeck coefficient observed to be high along the b axis and in the range 251 $\mu\text{V/K}$ at 300 K to 249 $\mu\text{V/K}$ at 800 K.
- On the a axis the Seebeck coefficient observed to be higher than the c axis and decreases with temperature from 245 $\mu\text{V/K}$ at 300K to 236 $\mu\text{V/K}$ then rises to 242 $\mu\text{V/K}$ at 800¹³ K.

Conclusion

- Band structure was calculated and a band gap of 0.625 eV was found which was slightly lower compared to the experimental band gap of 0.9 eV
- Electrical conductivity (σ) was found to be high along the a & c axes and increased significantly with temperature from $1.233 \times 10^{18} \Omega^{-1}\text{ms}$ at 300 K to $4.897 \times 10^{18} / \Omega \text{ ms}$ at 800 K along the a-axis and from (1.416×10^{18} to $6.49 \times 10^{18} \Omega^{-1} \text{ ms}$) along the c axis.
- Electronic thermal conductivity (K_e) was found to be low along the a- axis ($8.403 \times 10^{12} \text{ W/mKs}$ at 300 K to $1.073 \times 10^{14} \text{ W/mKs}$ at 800 K).
- Seebeck coefficient (S) was found to be in the range $234 \mu\text{V/K}$ to $251 \mu\text{V/K}$ across all axes between 300 K to 800 K which is sufficiently large enough for thermoelectric applications.

References

1. Giannozzi, P., Baroni, S., Bonini, N., Calandra, M., Car, R., Cavazzoni, C., Ceresoli, D., Chiarotti, G. L., Cococcioni, M., Dabo, I., Dal Corso, A., De Gironcoli, S., Fabris, S., Fratesi, G., Gebauer, R., Gerstmann, U., Gougoussis, C., Kokalj, A., Lazzeri, M., ... Wentzcovitch, R. M. (2009). Quantum espresso: A modular and open-source software project for quantum simulations of materials. *Journal of Physics: Condensed Matter*, 21(39), 395502. <https://doi.org/10.1088/0953-8984/21/39/395502>
2. Shi, Weiran et al. 2018. “Tin Selenide (τ)SnSe): Growth, Properties, and Applications.” 1700602.
3. Huang, Y., Wang, C., Chen, X., Zhou, D., Du, J., Wang, S., & Ning, L. (2017). RSC Advances First-principles study on intrinsic defects of SnSe. 27612–27618. <https://doi.org/10.1039/c7ra03367b>
4. Kresse, G., & Joubert, D. (1999). From ultrasoft pseudopotentials to the projector augmented-wave method. *Physical Review B*, 59(3), 1758-1775. <https://doi.org/10.1103/physrevb.59.1758>
5. Kumar, N., Bathula, S., Gahtori, B., Tyagi, K., Haranath, D., & Dhar, A. (2016). The effect of doping on thermoelectric performance of p-type SnSe : Promising thermoelectric material. *Journal of Alloys and Compounds*, 668, 152–158. <https://doi.org/10.1016/j.jallcom.2016.01.190>
6. Lundstrom, M. (2009). *Fundamentals of carrier transport*. Cambridge University Press.
7. Madsen, G. K., & Singh, D. J. (2006). BoltzTraP. A code for calculating band-structure dependent quantities. *Computer Physics communications*, 175(1), 67-71. <https://doi.org/10.1016/j.cpc.2006.03.007>
8. Sholl, D., & Steckel, J.A (2009). *Density functional theory: A practical introduction*. John Wiley and Sons.
9. Thermoelectric.(n.d). NETZSCH Analyzing & Testing. <https://www.netzsch.com/n47875>

Acknowledgements

- Center for High Performance Computing (CHPC-MATS862) for computational resources.
- The Materials Modeling Group of the Technical University of Kenya; <http://spas.tukenya.ac.ke/>
- My Supervisor and academic advisor.

Materials Modeling Group



THANK YOU!